High-contrast 40 Gb/s operation of a 500 μm long silicon carrier-depletion slow wave modulator

A. Brimont,[1,*] D. J. Thomson,[2] F. Y. Gardes,[2] J. M. Fedeli,[3] G. T. Reed,[2] J. Martí,[1] and P. Sanchis[1]

[1]*Nanophotonics Technology Center, Universitat Politècnica de Valencia, Camino de Vera s/n 46022 Valencia, Spain*

[2]*School of Electronics and Computer Science, University of Southampton, Southampton, UK*

[3]*CEA, LETI, Minatec Campus, 17 Rue des Martyrs, 38054 GRENOBLE Cedex, France*

**Corresponding author: abrimont@ntc.upv.es*

Received May 23, 2012; revised July 6, 2012; accepted July 6, 2012;
posted July 6, 2012 (Doc. ID 169068); published August 17, 2012

In this Letter, we demonstrate a highly efficient, compact, high-contrast and low-loss silicon slow wave modulator based on a traveling-wave Mach–Zehnder interferometer with two 500 μm long slow wave phase shifters. 40 Gb/s operation with 6.6 dB extinction ratio at quadrature and with an on-chip insertion loss of only 6 dB is shown. These results confirm the benefits of slow light as a means to enhance the performance of silicon modulators based on the plasma dispersion effect.

OCIS codes: 130.0130, 130.4110, 130.5296.

Among the variety of building blocks required to assemble future low-cost transceivers, an ever-growing attention has been given to silicon modulators over the last few years. Despite the constant endeavor toward the realization of high-performance devices, carrier-depletion modulators persistently find themselves facing parametric-adjustment trade-offs. As a result, building a modulator that simultaneously features high speed (40 Gb/s), small footprint (a few hundred micrometers), low insertion loss (IL) (<6 dB), and low drive voltage (~1 V) appears to be more challenging than initially thought [1–6]. It is now increasingly believed that the use of slow light may help mitigate these trade-offs. As a matter of fact, slow light was foreseen [7] and more recently shown [4,8] as providing an exciting opportunity to significantly enhance conventional "fast light" devices for numerous applications ranging from telecom and datacom to sensing via enlarged light-matter interactions. This paper aims to plainly showcase the advantages of slow light via demonstrating a highly efficient, compact, high-contrast, and low-loss silicon slow wave modulator.

Figures 1(a) and 1(b) show the schematic of the slow wave modulator along with a scanning electron microscope (SEM) picture of the fabricated traveling wave (TW) electrodes. Both arms of the Mach–Zehnder interface (MZI) consist of two identical 500 μm long slow wave phase shifters to balance the optical power and thus maximize the notch depth. An extra 900 μm long rib waveguide section has been added on one arm of the MZI to allow the operating point of the modulator to be precisely set. As shown in Fig. 1(c), slow light propagation is achieved through the use of a laterally corrugated waveguide, with narrow and wide sections of width $W = 300$ nm and $W_e = 650$ nm, which are repeated over a period $a = 310$ nm. The slow wave waveguide height is 220 nm. A partial dry-etching process is used to define the rib waveguide, leaving a 100 nm thick slab. More details on the slow light mode features may be found in [9]. Optical phase modulation is achieved by depleting the majority carriers from a reverse-biased p-n junction positioned in the middle of the waveguide and connected to highly doped p^+ and n^+ regions. As depicted in Fig. 1(c), these are situated respectively at a distance of $S_n = 550$ nm and $S_p = 500$ nm from the edge of the narrow waveguide section and metalized with compound AlCu electrodes as shown in Fig. 1(d). Net doping concentrations in the p- and n- type regions reached respectively 4×10^{17} cm^{-3} and 5×10^{17} cm^{-3}. Highly p^+ and n^+ doped regions were implanted, both at a concentration of 1×10^{20} cm^{-3}.

To assess the performance of the slow light modulator, a careful DC characterization process has been carried out. Figure 2(a) shows the optical spectra of both the MZI modulator and the corresponding 500 μm long phase shifter. Both spectra were normalized with a straight waveguide of identical length containing the same number of bends and tapers. As can be observed on the right-hand side of Fig. 2(a), the loss of the single slow light phase shifter in the fast light region ($n_g \sim 4.4$) lies around 1.5 dB and gradually increases as we move toward the slow light region. Because the group index dependence cannot be directly extracted from the interference

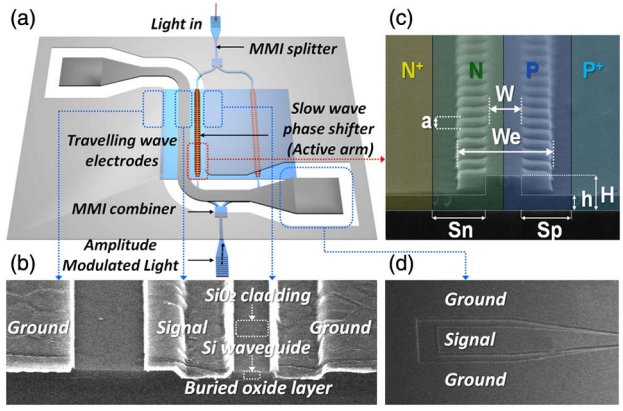

Fig. 1. (Color online) (a) Schematic of the slow wave modulator, SEM pictures of (b) the traveling wave coplanar electrodes, (c) the corrugated waveguide, and (d) the contacting AlCu pads.

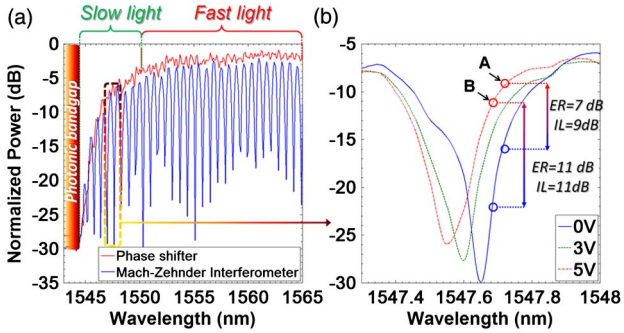

Fig. 2. (Color online) (a) Respective normalized spectra of the phase shifter (red curve, top) and the MZI (blue curve, bottom); (b) close-up view of the MZI spectrum for reverse biases of 0 V, −3 V, and −5 V.

fringes of this MZI because both arms contain identical phase shifters, an asymmetric version was simultaneously characterized so the group index could be extracted from the free spectral range variations across wavelength [4]. Figure 2(b) depicts a close-up portion of the slow light region ($n_g \sim 8$) of the MZI modulator under reverse bias voltages varying between 0 V, −3 V, and −5 V. The maximum transmission of the MZI is situated around −6 dB at 0 V, corresponding to a net on-chip loss of 6 dB, from which 5 dB arise from the slow wave phase shifter (coupling loss and propagation loss included) and 1 dB is due to the tapered multimode interference (MMI) structures (0.5 dB/MMI). As can be observed, a DC extinction ratio [referred to as ER in Fig. 2(b)] of ∼7 dB may be achieved at the quadrature point, designated "A" and located at 1547.7 nm wavelength. At this point, the maximum transmission is situated at −9 dB, which means that the IL penalty at the "1 1evel" is 9 dB, including the 1 dB loss arising from the two MMIs. The latter is extracted from the difference between the two curves shown in Fig 2(a). With an additional loss penalty of 2 dB (point B), leading to an overall IL of 11 dB, the extinction ratio increases up to ∼11 dB.

Additionally, the effective index change as a function of the applied reverse bias has been determined experimentally and supported by numerical calculations based on Soref and Bennett's empirical equations [10].

Figure 3 confirms that both experimental and numerical calculations are in good agreement, regardless of the

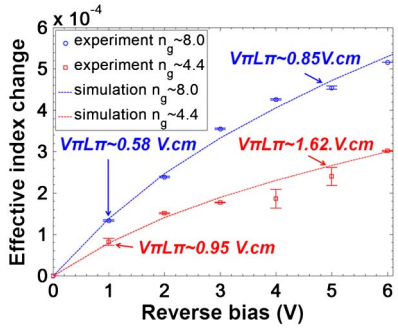

Fig. 3. (Color online) Effective index change versus reverse bias for group index values of ∼4.4 (fast light; red curve) and ∼8 (slow light; blue curve). Modulation efficiencies $V_\pi L_\pi$ are pointed by the arrows.

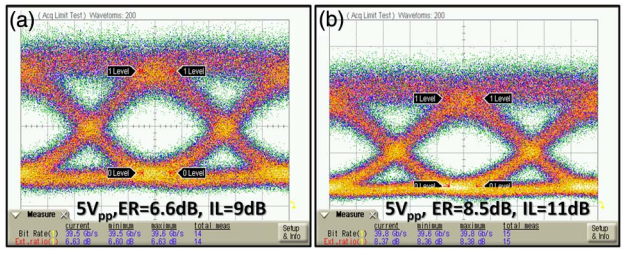

Fig. 4. (Color online) 40 Gb/s eye diagram (a) at quadrature and (b) 2 dB below quadrature.

small variations that may appear owing to the error in determining the notch shift across wavelength for varying reverse bias voltage. A clear enhancement of the modulation efficiencies ($V_\pi L_\pi$) between the fast ($n_g \sim 4.4$) and slow ($n_g \sim 8$) light regimes may be observed. It should be noticed that even in the fast light regime, the slight increase in group index compared to a conventional rib waveguide ($n_g \sim 3.8$) already provides a small but noticeable enhancement, as was demonstrated in our previous work [4] and in [11].

Overall, for a group index of ∼8, the modulation efficiency is improved by a factor of ∼2 compared to a conventional silicon modulator with identical doping conditions. In the slow light regime ($n_g \sim 8$), experimental modulation efficiencies of 0.58 V · cm and 0.85 V · cm for reverse biases of 1 V and 5 V were respectively calculated. By contrast, in the fast light regime ($n_g \sim 4.4$), modulation efficiencies of 0.95 V · cm and 1.62 V · cm were extracted for the same corresponding reverse biases.

To evaluate the high-speed performance of the slow wave modulator, 40 Gb/s eye diagram acquisitions at quadrature and 2 dB below quadrature were carried out under a $5V_{pp}$ drive voltage, as respectively depicted in Figs. 4(a) and 4(b). A full description of the setup is given in our previous work [4].

Consistently with our prior DC measurements, the measured extinction ratios are 6.6 dB and 8.5 dB at quadrature and 2 dB below quadrature, respectively.

One should be aware that the group index at which the modulator is operated is slightly lower ($n_g \sim 8$) than that used in our previous work ($n_g \sim 11$) [4]. Besides the lower optical losses, the choice of using such a group index value is motivated by the possibility of achieving a better electro-optical velocity matching and thus a higher modulation bandwidth. Although additional effects such as the microwave attenuation and impedance mismatch also contribute to the bandwidth reduction, the velocity mismatch between the electrical and optical signals plays a major role, especially as the group index increases [4]. However, it is important to remark that to sustain the performance in terms of extinction ratio, the phase shifter length maybe reduced according to the increase in group index. In this way, the higher velocity mismatch is partly counteracted by the shorter electro-optical interaction length.

On the other hand, the optical bandwidth of our slow light modulator, defined as the wavelength range over which the group index variations remain within 10% of the target value [9], is around 1.3 nm [4]. Although this

Table 1. Performance Comparison of Previously Reported 40 Gb/s Silicon Modulators, Including Our Work[a]

Reference	Year	Electrical Structure	$V_\pi L_\pi$	V_{pp}	ER@ 40 Gb/s	On-Chip IL	Optical Loss@ 40 Gb/s	PS Length
[1]	2007	Vertical pn	4 V · cm	6.5 V	1 dB	4 dB	–	1.0 mm
[2]	2011	Wrapped around pn	11–14 V · cm	6 V	6.5 dB	15 dB	25 dB	1.35 mm
[3]	2011	Self-aligned pn	2.7 V · cm	6.5 V	10 dB	15 dB	15 dB	3.5 mm
[3]	2011	Self-aligned pn	2.7 V · cm	6.5 V	7.5 dB	5 dB	8 dB	1.0 mm
[4]	2011	Self-aligned pn	1.27 V · cm[b]	5 V	3 dB	10 dB	13 dB	0. 5 mm
[5]	2012	Horizontal pipin	3.5 V · cm	6–7 V	3.2 dB	2. 5 dB	4.5 dB	0.95 mm
[5]	2012	Horizontal pipin	3.5 V · cm	6–7 V	6.6 dB	6 dB	6 dB	4.7 mm
[6]	2012	Horizontal pn	2.4 V · cm	5.2 V	6 dB	6.6 dB	–	4.0 mm
Our work	**2012**	**Horizontal pn**	**0.85 V · cm[c]**	**5 V**	**6.6 dB**	**6 dB**	**9 dB**	**0.5 mm**
Our work	**2012**	**Horizontal pn**	**0.85 V · cm[c]**	**5 V**	**8.5 dB**	**6 dB**	**11 dB**	**0.5 mm**

[a]ER = extinction ratio; IL = insertionloss; PS = phaseshifter.
[b]Modulation efficiencies for group indices of ∼11.
[c]Modulation efficiencies for group indices of ∼8.

value is far inferior to that of conventional MZI modulators (∼20–30 nm), it is much superior to resonantly enhanced devices based on high-Q ring resonators (<0.2 nm) [12]. The last challenge that will definitely allow slow light to win its spurs is showing a sustained performance over a broad optical bandwidth using engineered slow-light structures [9].

Interestingly, the relatively low optical loss value positions our slow light modulator among the state of the art of current 40 Gb/s modulators from an insertion loss and footprint point of view. As may be seen in Table 1, conventional MZI modulators featuring high extinction ratios (>6 dB) at 40 Gb/s require generally large footprints [3,5,6] (>3.5 mm) unless the operating point is close to minimum transmission [2], which results in turn in large optical losses (>15 dB). As an alternative, decreasing the footprint to reduce the on-chip IL (<6 dB) causes the extinction ratio to be reduced to around 3 dB [5] and below [1] unless the loss penalty increases with respect to the maximum transmission [3]. Overall, although tremendous efforts have been carried out over the last years, the trade-off between footprint, IL, and extinction ratio inherent to carrier depletion modulators seems to persist. This is why we believe that slow light is an attractive route to solve these issues while keeping the on-chip losses comparable to the state-of-the-art realizations reported so far, to our knowledge.

In conclusion, we have demonstrated high-contrast 40 Gb/s operation in a compact and low-loss slow light modulator. The device features an on-chip IL of only 6 dB, including the 1 dB loss of the two MMI structures. The enhanced modulation efficiency (0.85 V · cm) enabled 40 Gb/s data transmission with 6.6 dB extinction ratio (respectively, 8.5 dB) achieved at quadrature (respectively, 2 dB below quadrature) and with 9 dB (respectively, 11 dB) optical loss in a MZI with two identical 500 μm long phase shifters. We believe these results provide significant improvements in the field of silicon modulators at large, showing that slow light brings once more exciting prospects for silicon photonics.

Funding by the European Commission (EC) under project Photonics Electronics Functional Integration on CMOS (HELIOS) (FP7224312) and PROMETEO-2010-087 R&D Excellency Program are acknowledged. F.Y.G, D.J.T. and G.T.R. acknowledge funding support from the United Kingdom Engineering and Physical Sciences Research Council (EPSRC) under the grant "UK Silicon Photonics".

References

1. L. Liao, A. Liu, J. Basak, H. Nguyen, M. Paniccia, D. Rubin, Y. Chetrit, R. Cohen, and N. Izhaky, Electron. Lett. **43**, 1196 (2007).
2. F. Y. Gardes, D. J. Thomson, N. G. Emerson, and G. T. Reed, Opt. Express **19**, 11804 (2011).
3. D. J. Thomson, F. Y. Gardes, Y. Hu, G. Mashanovich, M. Fournier, P. Grosse, J. M. Fedeli, and G. T. Reed, Opt. Express **19**, 11507 (2011).
4. A. Brimont, D. J. Thomson, P. Sanchis, J. Herrera, F. Y. Gardes, J. M. Fedeli, G. T. Reed, and J. Martí, Opt. Express **19**, 20876 (2011).
5. M. Ziebell, D. Marris-Morini, G. Rasigade, J.-M. Fédéli, P. Crozat, E. Cassan, D. Bouville, and L. Vivien, Opt. Express **20**, 10591 (2012).
6. P. Dong, L. Chen, and Y.-K. Chen, Opt. Express **20**, 6163 (2012).
7. H. F. Taylor, J. Lightwave Technol. **17**, 1875 (1999).
8. L. O'Faolain, D. M. Beggs, T. P. White, T. Kampfrath, K. Kuipers, and T. F. Krauss, IEEE Photon. J. **2**, 404 (2010).
9. A. Brimont, J. V. Galán, J. M. Escalante, J. Martí, and P. Sanchis, Opt. Lett. **35**, 2708 (2010).
10. R. A. Soref and B. R. Bennett, IEEE J. Quantum Electron. **23**, 123 (1987).
11. H. C. Nguyen, Y. Sakai, M. Shinkawa, N. Ishikura, and T. Baba, Opt. Express **19**, 13000 (2011).
12. P. Dong, S. Liao, H. Liang, W. Qian, X. Wang, R. Shafiiha, D. Feng, G. Li, X. Zheng, A. V. Krishnamoorthy, and M. Asghari, Opt. Lett. **35**, 3246 (2010).